Atoms in axially-shifted tightly focused counter-propagating beams: the role of the Gouy and curvature phases

K. KOKSAL[1,2,*], V. E. LEMBESSIS[3], J. YUAN[2], AND M. BABIKER[2]

[1] Physics Department, Bitlis Eren University, Bitlis 13000, Turkey
[2] Department of Physics, University of York, Heslington, York YO10 5DD, England
[3] Quantum Technology Group, Department of Physics and Astronomy, College of Science, King Saud University, Riyadh 11451, Saudi Arabia
[*] Corresponding author: kkoksal@beu.edu.tr

Compiled June 23, 2020

We consider the interaction of atoms with two tightly focused and axially-shifted counter-propagating optical beams. At sub-wavelength focusing, we find that the scattering force potential in the three-dimensional space between the shifted focal planes changes from a feature with a saddle-point to a three-dimensional trapping potential. Further analysis shows that due to the tight focusing, the trapping depends on significant contributions arising from the Gouy and curvature phase gradients of the interfering beams. The physics and its effects are illustrated with reference to the sub-wavelength trapping of sodium atoms.

http://dx.doi.org/10.1364/ao.XX.XXXXXX

1. INTRODUCTION

One of the most striking effects of laser light is enabling the cooling and trapping of atoms [1, 2] and this led to the emergence of cold atom science which is now considered an important and integral part of many quantum technology developments. Atom trapping was first experimentally realised and explained as due to the optical dipole force [3] arising from the interaction of atoms with laser light whose frequency was carefully detuned from the atomic resonance. The scattering force was used to provide atom cooling [4], but it has also featured in some hybrid atom trapping schemes. However, this trapping was made possible only when the scattering force acted in conjunction with either a magnetic field [5] or with the optical dipole force [3, 6].

The trapping of atoms by the optical dipole force and their cooling by the scattering force constitute the main approach in the optical control of the atoms [1, 7, 8]. The recent work by Mashimo et al [9] on the trapping of rubidium atoms employed both types of force. On the other hand, the use of magnetic fields involves bulky instrumentation, so an all-optical trapping scheme for atoms and nanoparticles would provide simplicity and ease of control as well as the added possibility of combining trapping with efficient cooling.

In the early days of laser cooling and trapping Ashkin [10] drew attention to the Optical Earnshaw Theorem (OET) which was put forward in analogy with the well-known electrostatic Earnshaw Theorem [11]. The theorem states that a small dielectric sphere, acting as a polarization dipole, cannot be trapped in a three-dimensional region of space purely by using the optical scattering force. As a result some effort has been focused on circumventing OET, for example, either by using a time-dependent radiation force [12] which increases the complexity of the system, or the dipole radiation force at near-resonance which is typically a weak force. For an account on the scattering force in the context of atom trapping, see the recent article by Sukhov [13].

Most work on laser cooling and trapping of atoms has dealt with fairly broad beams but recent developments have led to the generation and the application of optical beams that are focused to sub-wavelength sizes [14–16]. Dorn et al [17] demonstrated experimentally that a radially polarized field can be focused to a spot size significantly smaller ($0.16\lambda^2$) than for a linearly polarized field ($0.26\lambda^2$). Accounts of recent developments on the sharp focusing of laser light can be found in the recent book by Kotlyar et al [18].

In this paper, we consider a scheme in which an optical environment is generated by two tightly focused but, significantly, axially-shifted counter-propagating optical beams. At sub-wavelength focusing we find that the scattering force potential in the region between the focal planes changes from a feature with a saddle-point to a three-dimensional trapping potential. Further analysis shows that the trapping arises with influences from contributions due to the Gouy and curvature phase gradients of the individual

beams . The physics and its effects are illustrated with reference to the trapping of sodium atoms. Our key finding is that the sub-wavelength focused light field arising from the interference of two axially-shifted counter-propagating beams, gives rise to a substantial three-dimensional optical trap with its center located at a point midway between the shifted focal planes. This all-optical trap is due solely to the scattering force when light is coupled at near resonance with the atomic transition. When compared with the corresponding dipole force due to light detuned far from resonance, it is found that the scattering force has the advantage of being much stronger and it can achieve the same magnitude of trapping potential as the dipole force but with a much weaker beam intensity.

The paper is organised as follows. In section 2 we outline the basics of the scattering force due to an arbitrary light field environment. Section 3 deals with the essential formalism for an optical focused light beam characterised by an amplitude function and a phase function. It then deals with the specification of the total field due to the interference of two counter-propagating axially shifted beams and we distinguish between two types of configuration in which the beams are separated so that their focal planes are face to face or back to back. Section 4 deals with the evaluation of the scattering force and the demonstration that at tight focusing a three-dimensional trap due solely to the scattering force is achievable. Section 5 deals with the low-intensity regime where the main aim is to explore the factors that enable the three-dimensional trapping to be realised due to significant contributions from the Gouy and curvature phases which come into play under tight focusing conditions. Section 6 contains our comments and final conclusions where we comment, in particular, on the challenges that are likely to be faced by an experimental realisation of an all-optical trapped under tight focusing conditions. However, as we pointed out earlier there are recent advances in the realisation of sub-wavelength focusing of light , but there are issues concerning laser jitter and beam misalignments effects which can be minimised using for example, adaptive optics approach techniques. We also point out using order of magnitude analysis in the light of our results for three-dimensional trapping that our scheme is capable of both efficient cooling of an atomic cloud as well its strong trapping and at low intensity.

2. THE OPTICAL SCATTERING FORCE

Ashkin [10] showed that for a particle with a constant linear polarisability, the divergence of the scattering force is zero ($\vec{\nabla}\cdot <\vec{F}>=0$). This means that the optical potential experienced by the particle has a saddle-point as a major feature and so excludes the possibility of trapping a polarisable particle using the scattering force alone, as the force lines pointing towards any point are balanced by the outgoing force lines from the same position over a complete surface around the saddle point. However, this conclusion was based on the fact that the particle polarisability is a constant [10] and that the fields are assumed to be exact solutions of the Helmholtz equation. Nevertheless, it is well known that for a two-level neutral atom (as a point-like dielectric particle), the assumption of a constant polarisability is not valid when the atom is driven coherently under near-resonance conditions [19].

Near resonance, one has to take account of the Rabi oscillations of the occupancy of the two levels of the atom [19, 20]. Defining $\Omega_R = \frac{|\vec{\mu}\cdot\hat{e}E(\vec{r})|}{\hbar}$) as the Rabi frequency, μ the transition dipole matrix element and $\hat{e}$ the polarisation vector of the applied electric field, the scattering force can be cast in the form [8, 10, 20]:

$$<\vec{F}_{sca}>=\left[\hbar\vec{\nabla}\Theta\right]\Gamma\frac{\Omega_R^2}{4(\Delta_0^2+\Omega_R^2/2+\Gamma^2/4)}. \tag{1}$$

where Θ is the phase function, $\Delta_0=\omega-\omega_0$ is the detuning, and Γ is the spontaneous decay rate.

The scattering force can be written in terms of the more familiar saturation parameter $s=\frac{\Omega_R^2/2}{\Delta_0{}^2+\Gamma^2/4}$ as follows [19]

$$<\vec{F}_{sca}>=\frac{\hbar\Gamma}{2}\frac{s}{1+s}\vec{\nabla}\Theta. \tag{2}$$

Since the saturation parameter s is not a constant, as it depends on the square of the Rabi frequency Ω_R which is a function of position, the divergence of the scattering force in Eqn.(2) is clearly non-zero in general. This leads to the prospect of the creation of a three-dimensional optical trap which is solely due to the scattering force.

For small s the scattering force can be written as

$$<\vec{F}_{sca}>\approx\frac{\hbar\Gamma}{2}(s\vec{\nabla}\Theta) \tag{3}$$

It is straightforward to deduce from Eqn.(2) that at full saturation ($s>>1$), the scattering force is independent of the intensity and is given by $\hbar\Gamma\vec{\nabla}\Theta/2$. Taking the divergence we have

$$\vec{\nabla}\cdot<\vec{F}_{\rm sca}>=\vec{\nabla}\cdot\left(\frac{\hbar\Gamma}{2}\vec{\nabla}\Theta)\right)=\frac{\hbar\Gamma}{2}\nabla^2\Theta \tag{4}$$

This special result, applicable at high saturation, suggests that we may associate the scattering force with an effective 'potential' proportional to $-\Theta$. In that case, our condition for three-dimensional trapping by scattering force is equivalent to a negative curvature of the 'potential', which is consistent with the existence of a trap. However, the dependence of the scattering force in Eqn.(2) on the saturation function s implies that we have to examine the direction and magnitude of the force in order to ascertain trapping features.

3. THE OPTICAL FIELD ENVIRONMENT

A. Beam amplitude and phase functions

The optical configuration we focus on here consists of a pair of axially-shifted Gaussian beams each characterised by the same frequency ω and axial wave-vector k. in order to specify the total amplitude function and the phase function of the configuration we begin by outlining the formalism for one beam travelling along the positive z-axis in terms of the cylindrical space coordinates $\mathbf{r} = (\rho, \phi, z)$. The electric field amplitude function for light linearly polarised along $\hat{\epsilon}$ is as follows

$$\vec{E}(\vec{r}, t) = E(\rho, z, t) e^{i\theta(\rho,z)} \hat{\epsilon} \tag{5}$$

where $E(\rho, z, t)$ is the amplitude function

$$E(\rho, z, t) = \mathcal{E} \frac{1}{\sqrt{1 + \frac{z^2}{z_R^2}}} e^{-\frac{\rho^2}{w^2(z)}} e^{-i\omega t}, \tag{6}$$

where $\mathcal{E}$ is a constant and $\theta(\rho, z)$ is the phase function

$$\theta = kz + \theta_{Gouy} + \theta_{curv}, \tag{7}$$

with

$$\theta_{Gouy} = -\tan^{-1}(z/z_R); \qquad \theta_{curv} = \frac{k\rho^2 z}{2(z^2 + z_R^2)}. \tag{8}$$

The first term in the phase function is the usual term representing plane wave propagation with axial wave-vector k. The second term is the Gouy phase and the final term enters as a phase contribution due to the variation of the beam curvature with axial position z. In the equations above $w(z)$ is the beam waist at axial coordinate z such that $w^2(z) = 2(z^2 + z_R^2)/kz_R$, where z_R is the Rayleigh range. w_0 is the waist radius at the focal plane. The above formalism can be easily adapted to define the amplitude and phase functions of a counter-propagating beam travelling along the negative z-axis. In addition, simple space transformation along the common axis will allow us to express the functions in the situation where the focal planes are shifted relative to each other.

B. Two distinct beam configurations

As pointed out, Eqn. (2) is not sufficient to ensure a three-dimensional trap due to the scattering force alone. We also have to make sure that the force distribution vectors point towards the same trapping point in space. Here we demonstrate one such possibility using optical environments due to two lineally polarized, axially-shifted, counter-propagating and highly focused Gaussian beams (see Fig. 1). Such a geometry for broad beams has been discussed since the early days of atom optics [4, 5, 21, 22], as it results in counteracting axial forces associated with the individual beams. There has also been no proper analysis of the fields and the interaction in this configuration, including the manner of the interference of the counter-propagating beams, the effects of focal plane separation and the manner in which the two beams are counter-propagating, which, as we show here, brings to the fore the contributions from the Gouy and the curvature phases of the interfering beams. We show here that the additional phase structure introduced by the tightly focused axially shifted beams enables the creation of a trap based solely on the scattering force.

When the focusing is sufficiently tight the additional phase effects, including the Gouy and curvature phases become significant. With the two beams having the same polarisation $\hat{\epsilon}$, say along the $y-$axis, with propagation along the $z-$axis the field vector due to the individual beams are as follows

$$\vec{E}_1(\vec{r}) = E_{0,1}(\vec{r}) e^{i\theta_1(\vec{r})} \hat{\epsilon}; \qquad \vec{E}_2(\vec{r}) = E_{0,2} e^{i\theta_2(\vec{r})} \hat{\epsilon}, \tag{9}$$

where the amplitude functions $E_{0,1}$ and $E_{0,2}$ and phase function θ_1 and θ_2 follow the format given above for a general Gaussian light beam.

Since the individual interfering beam polarisations are the same the total field has a well defined overall amplitude function $E_0(\mathbf{r})$ and an overall phase function $\Theta(\mathbf{r})$, so that

$$\vec{E}(\vec{r}) = E_0(\vec{r}) e^{i\Theta(\vec{r})} \hat{\epsilon}, \tag{10}$$

By following our recent work [23], it is straightforward to show that $E_0(\mathbf{r})$ and $\Theta(\mathbf{r})$ are as follows

$$E_0(\vec{r}) = \sqrt{E_{0,1}^2(\vec{r}) + E_{0,2}^2(\vec{r}) + 2E_{0,1}(\vec{r}) E_{0,2}(\vec{r}) \cos\left(\theta_1(\vec{r}) - \theta_2(\vec{r})\right)} \tag{11}$$

and

$$\Theta(\vec{r}) = \tan^{-1}\left\{ \frac{E_{0,1}(\vec{r}) \sin\theta_1(\vec{r}) + E_{0,2}(\vec{r}) \sin\theta_2(\vec{r})}{E_{0,1}(\vec{r}) \cos\theta_1(\vec{r}) + E_{0,2}(\vec{r}) \cos\theta_2(\vec{r})} \right\} \tag{12}$$

With the the origin of coordinates taken to be at $z = 0$, we take the focal plane of beam 1(2) to coincide with the planes $z = -d/2(d/2)$ where $d > 0$. Expressions for the amplitudes and phase of individual beams are obtainable the general expressions Eqs. (6) to (8) are then specified by use of the transformation $z \to (z - d/2)$ for beam 1 and $z \to z + d/2$ for beam 2 as shown in Fig. 1. Note, however, that another distinctly different beam environment is obtainable when we consider the case $d < 0$. The configuration where $d > 0$ corresponds to beams propagating with focal plane 'arrows' pointing at each other (face to face), while the $d < 0$ they are referred to as back to back. Figure 1 schematically shows the two configurations which correspond to the cases $d > 0$ and $d < 0$. The most striking difference is that of the variation of the Gouy phase across the symmetry plane at $z = 0$. This difference is one of the factors controlling the possibility of the creation of a three-dimensional trap arising from the scattering force.

Note the intermixing of the phases and amplitudes of the individual beams to give rise to the total amplitudes and phase functions in Eqns. (11-12) in which the the spatial dependence of plays a significant role.

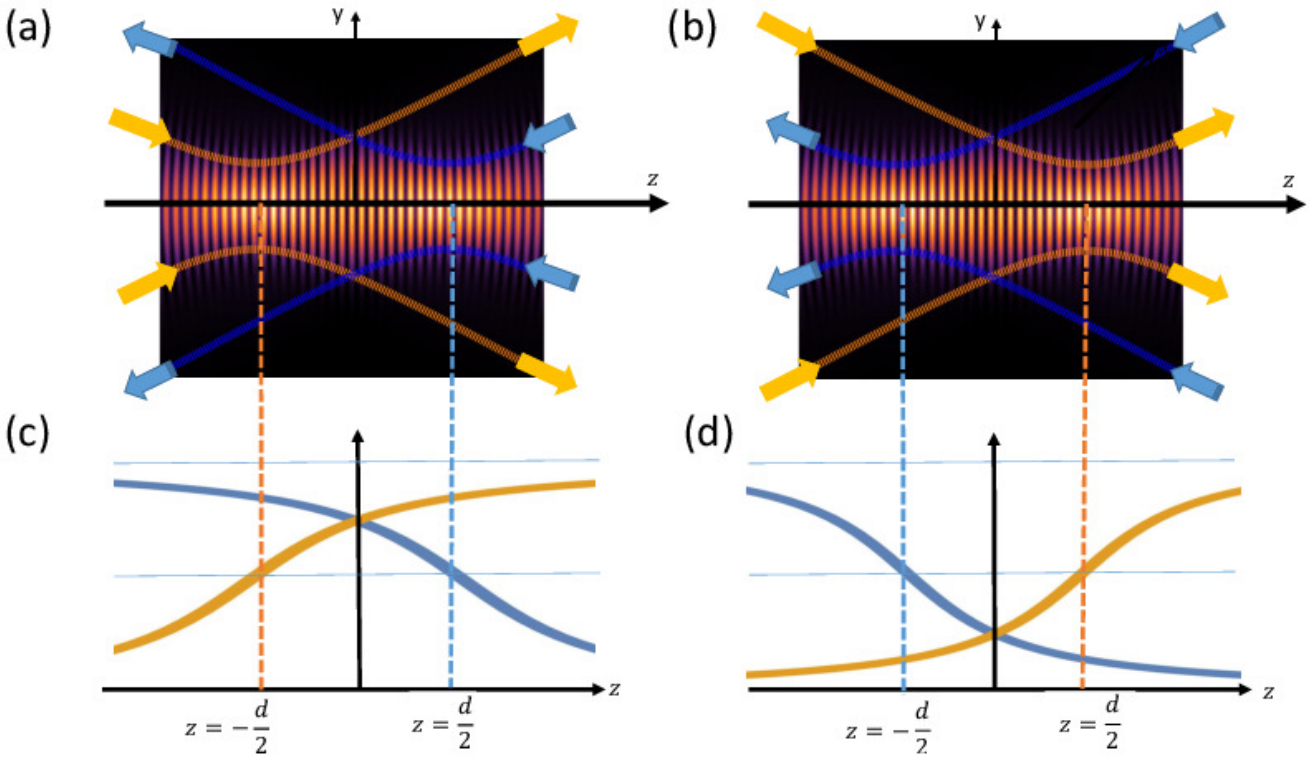

Fig. 1. Two counter-propagating focused Gaussian beams with a finite displacement d of the respective focal planes. In the left panel (a and c), the focal plane of the orange(blue) beam is located to the right(left) of the $z = 0$ plane. Alternatively, as shown in the right panel (b and d), the focal plane of the blue(orange) beam is located to the left(right) of the $z = 0$ plane. The two cases are related by interchanging d by $-d$. In the top row, only beam intensities are shown schematically which is symmetrical with respect to change in the sign of d. The bottom row shows the Gouy phases of the two beams and changes in the sign of d is related to a change of sign of the respective Gouy phases with respect to the $z = 0$ plane.

4. SCATTERING FORCE BETWEEN FOCAL PLANES

A. Force vector distribution

With the functional forms of the total amplitude and total phase determined as described above, the scattering force emerges by direct evaluation of Eqn. (2), which requires input of the total amplitude and phase functions, Eqs.(11) and (12)) along with suitable parameters.

The scattering force variation in terms of both magnitude and direction is shown in Fig. 2. This displays the results for two linearly polarized counter-propagating Gaussian beams with a narrow beam waist at $w_0 = 0.2\lambda$ and with the focal planes of the two counter-propagating beams axially shifted from each other by a distance of $d = +w_0$. It is clear from Fig. 2 that all the force vectors point towards the centre where the force amplitude is zero, so displaying all the hallmarks of a three-dimensional trap about the origin. Note that the shifting of the focal planes is crucial for the trapping. The total phase is zero if the two counter-propagating Gaussian beams are not axially shifted, as then the beam configuration corresponds to a standing wave of finite amplitude.

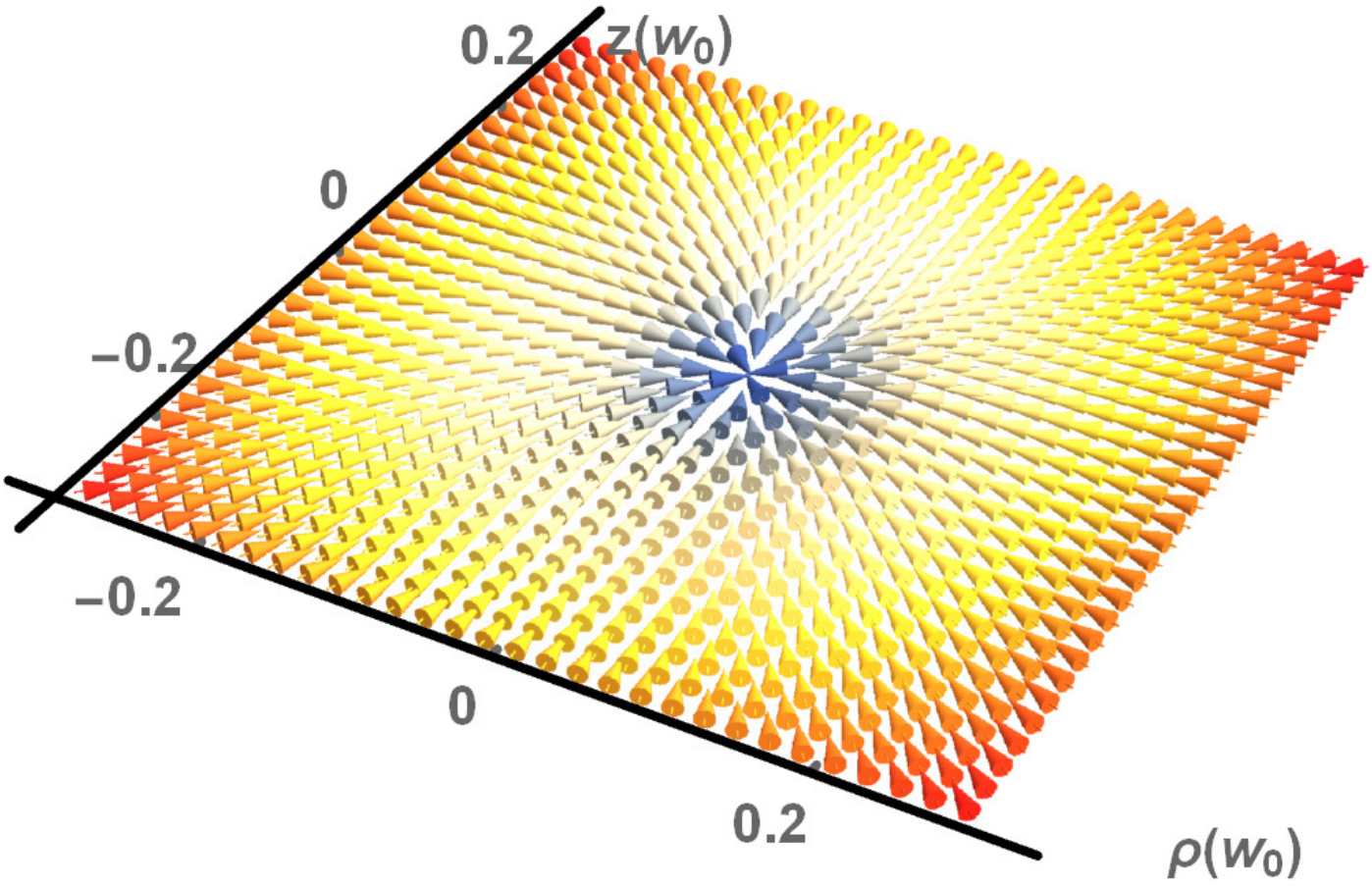

Fig. 2. The scattering force vector exhibiting the trapping of sodium atoms due to the scattering force in the interaction with the two counter-propagating axially shifted and tightly focused beams. The plot shows the region between the focal planes near the symmetry point $z = 0$ and $\rho = 0$. The Gaussian beam parameters used were:wavelength $\lambda = 589$ nm, beam waist $w_0 = 0.2\lambda$, light intensity $I = 64$ Wm^{-2} and distance between focal planes $d = -w_0$

An estimate of the maximum depth of the trapping potential can be made by examining its variations in the saturation limit $s >> 1$. This is plotted in Fig. 3 evaluated for Na atoms as the two-level system and with the parameters used to evaluate the potential shown in the caption to that figure. The potential (given in units of the sodium recoil energy $E_{rec} = \hbar^2k^2/2M$) has a depth that well exceeds E_{rec} [1]. It is well known that for efficient trapping the depth at minimum must be greater than the atomic recoil energy and we see from the figure that the trap is sufficiently deep to trap sodium atoms.

B. The two beam configurations and trapping

In order to understand the conditions necessary for the existence of an all-optical scattering force trap in the above situation we need to investigate its dependence on the beam configuration parameters, notably the beam waist (w_0), axial separation d between the focal planes of the two beams and the individual beam intensity I. As explained earlier, the axial separation d is defined to be either positive $d > 0$ if the two focal planes are short of the equilibrium position (so their propagation vectors face each other (face to face)),

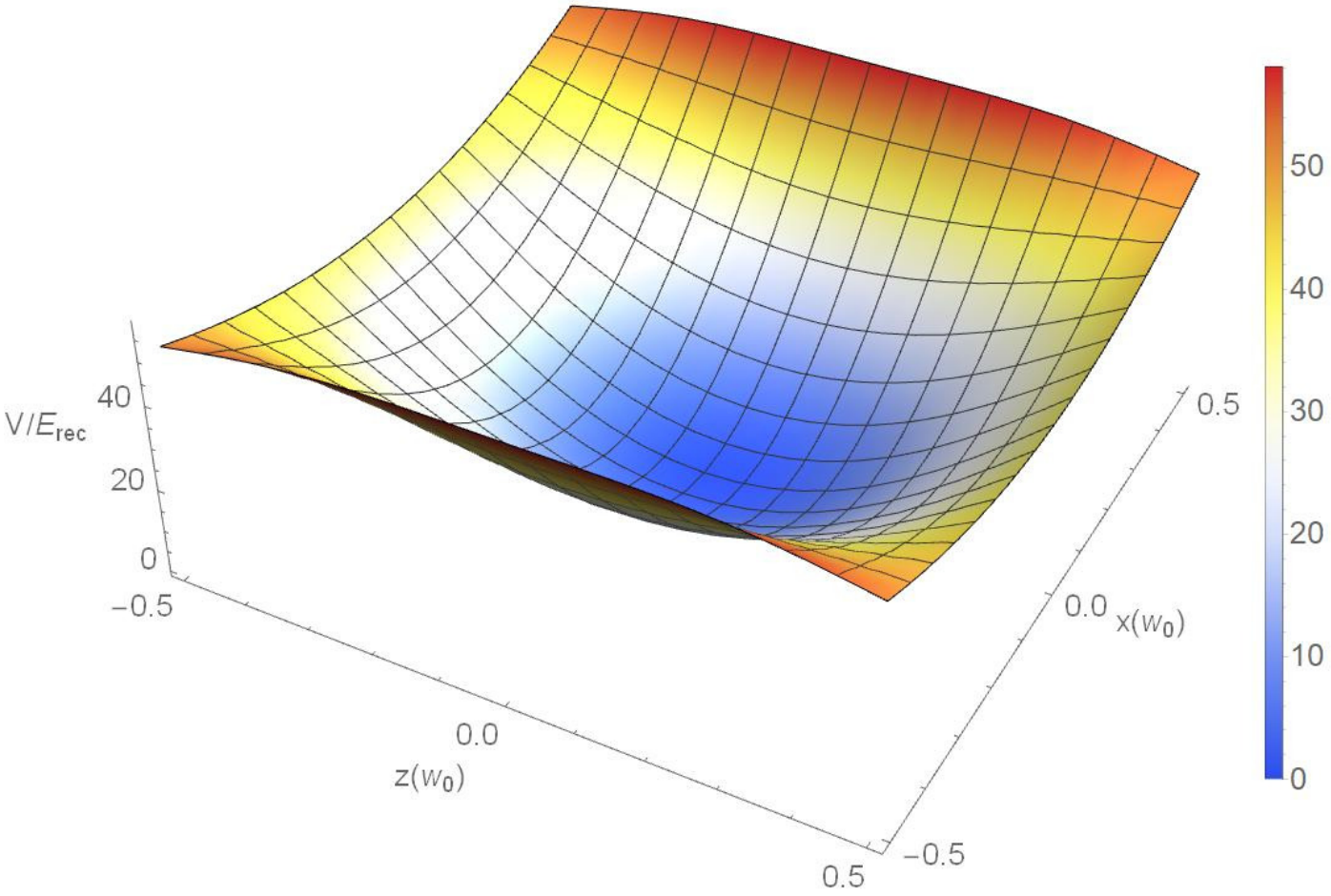

Fig. 3. The scattering force potential for sodium atoms in the field of the two axially shifted counter-propagating Gaussian beams at full saturation. The variations of the potential are shown in the region between the focal planes as a function of x, z and given in units of the sodium recoil energy E_{rec}. The parameters used in generating this plot are as follows: wavelength $\lambda = 589$ nm, beam waist $w_0 = 0.2\lambda$, light intensity $I = 64\ \mathrm{Wm}^{-2}$, distance between focal planes $d = -w_0$. The value of E_{rec} at wavelength $\lambda = 589$ nm is $E_{rec} = 1.6 \times 10^{-29}$ J [1].

or negative $d < 0$ if both focal planes are beyond the equilibrium position (so that their propagation vectors are away from each other (back to back)).

In the vicinity of the symmetry point $(\rho, z) = (0, 0))$ the scattering force axial and radial components can be represented in terms of force constants as follows

$$F_z = K_z z; \qquad F_\rho = K_\rho \rho \tag{13}$$

These are obtainable as the linear terms of the Taylor expansion of the scattering force about the equilibrium position at $(z = 0, \rho = 0)$. For three-dimensional trapping the signs of both K_z and K_ρ must be negative. In Fig. 4 we present the corresponding force constants for two representative beam waists (w_0). The results for the force constants shown in Fig.4(a,b) are typical of the situation when broad waist beams are employed. In the case when the propagation vectors are face to face (i.e. $d > 0$), we find that the radial force constant K_ρ is always positive while the axial force constant K_z is negative. This means that the atom would be trapped axially towards $z = 0$ but would be repelled radially from the axis $\rho = 0$. The signs of these two force constants are reversed for the case $d < 0$. Thus, in both cases, the scattering force is equivalent to the atom being effectively in a saddle-point potential.

Significantly different behaviour emerges, as shown in Fig. 4(c,d), when the beam waist is reduced so that each beam waist has a tightly focused value $w_0 = 0.2\lambda$. Here the axial force constant K_z exhibits oscillations as a function of d. For the case $d > 0$, the oscillations lead us to identify regions of d variation where the force constants change sign. At the smaller d range, both force constants K_ρ and K_z are positive, indicating a local potential maximum. For the large d values, the atom experiences a saddle-point-like effective potential. More significant results concern the situation where $d < 0$. Again we have two regions where the signs of K_z are opposite. In the small range of negative d, both the radial and axial force constants K_ρ and K_z are negative, indicating a true three-dimensional scattering force atom trap. Figs. 2 and 3 show cases of force and potential variations where the three-dimensional trapping occurs. For large negative d values, we again have two force constants of opposite signs, so this shows that the saturation and tight focus alone are not sufficient conditions to create a three-dimensional trapping that depends solely on the optical scattering force.

5. THE LOW INTENSITY/ INDEPENDENT BEAMS REGIME

In what follows we seek to clarify the underlying physics involved by examining the emerging trends of the scattering force applicable in the low beam intensity regime. We shall see that the availability of the analytical results helps to understand the underlying physics that also plays a role in the high beam intensity regime. At low intensity the saturation effects are negligible and the overall scattering force can be determined by the independent beam approximation. This allows us to clarify the separate roles played by the saturation effect and the Gouy and curvature phases and the effects of varying beam waist.

In the independent beam approximation, the force experienced by a two-level atom is the sum of the scattering forces due to individual beams. We have

$$\vec{F}_{\text{sca}} = \vec{F}_{\text{sca},1} + \vec{F}_{\text{sca},2} \tag{14}$$

In the vicinity of the symmetry point the z-component of this force is given by

$$\begin{aligned} F_{sca,z} &= \hbar k \Gamma \left[\Pi_1(z + d/2) - \Pi_2(z - d/2)\right] \\ &\sim \hbar k \Gamma d \frac{\partial \Pi}{\partial z}\Big|_{z=d/2} z \end{aligned} \tag{15}$$

where an expression of $\Pi_{1,2}$ can be deduced by inspection of Eqn.(1). At the symmetry plane $z = 0$, the scattering forces due to the two individual beams cancel out because the Rabi frequencies Ω_R have the same values. Away from this equilibrium plane, we can expand the Rabi frequency variation about the $z = 0$ plane and find that the terms between the square brackets combine to give a linear dependence on z (interpreted as due to imbalance between the beam intensities through the spatial variations of the individual Rabi frequencies of the beams). We can then write

$$F_{sca,z} = K_R z, \tag{16}$$

where

$$K_R = -\hbar k \frac{\Gamma}{2} d \frac{(\Delta_0^2 + \Gamma^2)\Omega_R^2\big|_{z=d/2}}{(\Delta_0^2 + \frac{1}{2}\Omega_R^2\big|_{z=d/2} + \Gamma^2/4)}. \tag{17}$$

Interestingly, this is a trapping force (for $d > 0$). It attains a maximum when d is of the order of the beam waist w_0. When the sign of d is inverted $(d < 0)$ it changes to a repulsive force along the z-direction. This is interpreted as due to the expected reversal of the balance of the forward and backward scattering forces. This is consistent with the conventional qualitative understanding based on the strong spatial variation of the intensity distribution of the two beams in the neighbourhood of their respective focal planes ([5, 24]).

However, we can show that this is not always the case for highly convergent Gaussian beams. If we increase the convergence of the Gaussian beam (corresponding to small values of the Rayleigh range z_R), we have to consider the full expression for the phase of each beam. The gradient of the phase is such that

$$\begin{aligned} \frac{1}{k}\vec{\nabla}\Theta &= (1 - \Phi_z)\hat{z} + \Phi_\rho \hat{\rho} \\ &= \left(1 - \frac{z_R}{k(z^2 + z_R^2)} + \frac{\rho^2(z_R^2 - z^2)}{2(z_R^2 + z^2)^2}\right)\hat{z} + \frac{\rho z}{\rho^2 + z^2}\hat{\rho}. \end{aligned} \tag{18}$$

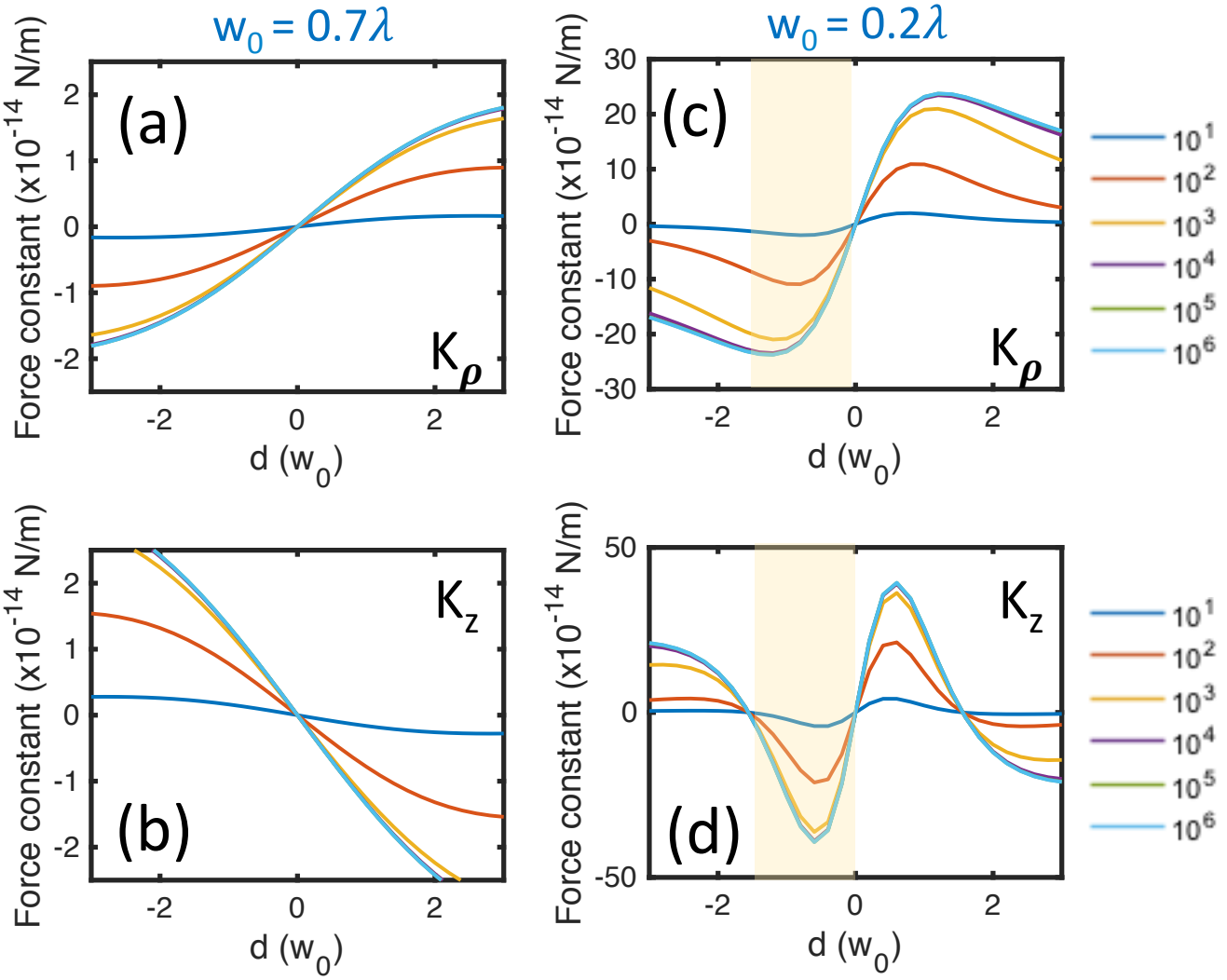

Fig. 4. The comparison of the variation of the force constants with the separation d between the focal planes for the scattering force due to two axially shifted counter-propagating beams. The variations are displayed by curves for different intensities as shown by different colours. Figures (a) and (b) show the d-dependence of the radial and axial force constants for relatively broad light beams, while figures (c), and (d) are as for (a) and (b) but with tightly focused beams. In the case shown in (a) and (b), three-dimensional trapping is not achievable, while in (c) and (d) three-dimensional trapping is achievable. The criteria for 3D trapping are such that both the radial force constant K_ρ and the axial force constant K_z are negative. These criteria are met in figures (c) and (d) which clearly show that both of the radial and the axial force constants are negative for a finite range of d<0.

where Φ_z and Φ_ρ are the changes in the phase gradients in the axial and radial directions, respectively. The z-component of the total scattering force is then:

$$\begin{aligned} F_{sca,z} =& \hbar k\Gamma \left[1-\Phi_z(z+d/2)\right]\Pi_1(z+d/2) \\ & -\hbar k\Gamma \left[1-\Phi_z(z-d/2)\right]\Pi_2(z-d/2). \end{aligned} \tag{19}$$

In the vicinity of the $z=0$ symmetry plane, we can expand the z-component of the force as a function of z and get:

$$\begin{aligned} F_{sca,z} &\sim \hbar k\Gamma d\left(\Phi(z=d/2)\frac{\partial\Pi}{\partial z}\Big|_{z=\frac{d}{2}} + \Pi(z=d/2)\frac{\partial\Phi}{\partial z}\Big|_{z=\frac{d}{2}}\right) \\ &= (K'_R - K_G)z = K_z z. \end{aligned} \tag{20}$$

where the force constants K'_R and K_G are as follows

$$K'_R = \left[1-\frac{z_R}{k(d^2/4+z_R^2)}\right]K_R \tag{21}$$

and

$$K_G = z_R\frac{\Delta_0^2+\Gamma^2/4+\Omega_0^2/2}{k(z_R^2+d^2/4)}K_R, \tag{22}$$

where k_R is given by Eqn. 17.

As z_R decreases, K_R increases while K_G decreases such that the net axial scattering force on axis can change from attractive to repulsive. However, off-axis, the axial force can still be attractive due to the contribution from the curvature phase which balances the negative effect of the Gouy phase shift. This means that the reversal effect is most significant for non-vortex Gaussian beams and creates the possibility of off-axis axial trapping separated by a repulsive on-axis barrier.

It turns out that the attractive potential for the case $d>0$ can be turned into a repulsive force for beams with small beam waist. However, both K_G and K'_R vary linearly with d while the derivative only contains d^2 terms, thus in the $d<0$ case, the sign of the force is inverted, changing from a repulsive potential at large beam waists to an attractive potential for small beam waists.

The change in the nature of the force can be physically understood as a change in the effective wavevector k_{eff} of the beam at the focal region due to the convergence of the beams. With the Gouy and beam curvature phase terms, we have for k_{eff} [25]

$$k_{eff} \sim k\left(1-\frac{1}{kz_R}+\frac{\rho^2}{2z_R^2}\right). \tag{23}$$

The second term in Eqn. 20 represents the scattering force due to an imbalance between different contributions to the effective wavevectors. The effective wavevector can, in principle, be reduced to zero or even take a negative value for Gaussian beams with large convergence, at least on the common beams' axis at $\rho=0$. At finite radial distance from the beam axis, the curvature phase contribution may cancel that due to the Gouy phase. This shows that the axial force acting on a two-level atom can change from attractive to repulsive off-axis.

The presence of the curvature phase term introduces a radial component to the scattering force:

$$F_{sca,\rho} = \hbar k\Gamma\Pi\Phi_\rho = \hbar k\Gamma\Pi\frac{\rho z}{z^2+z_R^2}. \tag{24}$$

In the $d<0$ case, the radial component of the net scattering force is given by:

$$F_{sca,\rho} = d\hbar k\Gamma\left(\frac{\partial\Pi}{\partial\rho}\Big|_{z=d/2}\Phi_\rho + \Pi\frac{\partial\Phi_\rho}{\partial\rho}\Big|_{z=d/2}\right). \tag{25}$$

Again, the first term is consistent with the conventional analysis of a repulsive force.

The above analysis suggests that a three-dimensional scattering force trap is possible if we can increase the Gouy phase contribution sufficiently to reverse the sign of the axial force in the $d<0$ case since we need the direction of the radial component of the scattering force to point inwards, which is only possible when $d<0$. In the axial direction, the difference in the beam intensities away from $z=0$ plane makes beam 1 dominant on the left side and beam 2 on the right side. This causes K_R to be positive (Eqn. 17). However, due to the Gouy phase term, there is a change in the size of the projected momentum along the z-direction which makes the beam 2 to be dominant on the left side and beam 1 on the right side of the $z=0$ plane. Note that the axial spring constant (K_R) is always positive, resulting in a repulsive contribution to the axial force, as pointed out earlier. The Gouy phase related axial component of the scattering force has a negative value spring constant ($-K_G$), so the net axial force can be changed. However, without the saturation effect that diminishes K_R preferentially in the high intensity light regime (mostly on axis), OET suggests that the difference is not sufficient to make $\vec{\nabla}\cdot\vec{F}_{sca}\neq 0$. Only by working under significant saturation and with a sufficiently large Gouy phase contribution, can we get the net spring constant $K_z = K'_R - K_G$ to reverse sign. As the Gouy phase change is largest within the beam focal planes, this reversal becomes significant at $d\leq w_0$. Our analysis also suggests that this occurs at very small z_R for a Gaussian beam and prompts us to also look into considering beams with a non-zero radial index, p. A value as large as $p=20$ should result in significant Gouy phase contributions at the larger beam waist. In their original paper on OET, Ashkin and Gordon [10] did not consider saturation effects on

the ground that they are detrimental to the formation and stability of any trap. Our analysis confirms this is true only when the Gouy phase is unimportant, i.e. when the beam-waist is large. This is because although the saturation effect weakens the scattering force, it could not on its own reverse its sign. We need the increased contribution of the Gouy phase which has an opposite sign to contribute to the reversal of the net axial scattering force. This means that the bypassing of OET is a necessary but not sufficient condition for the formation of three-dimensional all scattering force trap.

6. DISCUSSION AND CONCLUSIONS

We have presented a detailed analysis of the light field and the scattering force distribution on two-level atoms interacting with two axially-shifted counter-propagating tightly focused Gaussian beams. We have shown how such a configuration of focused light fields can lead to an optical trap due solely to the scattering force. Our further analytical work has shown that a large Gouy and curvature phase contributions in the region between the focal planes lead to a reduction of the axial repulsive scattering force. For a tightly focused beam this, in turn, leads to the a reversal of the sign of the axial scattering force and to the possibility of a three-dimensional trap for atoms. In the case of highly focused beams, further investigations will need to be made using non-paraxial beam solutions. However, the main differences between the paraxial and non-paraxial solutions of the beams are due to the presence of the axial component of the electric field vector for linearly polarised beams at a small beam waist [26]. For our chosen cases of counter-propagating beams, the z-component of the overall electric field is at most a few percents of the in-plane field components, rendering their contribution to the force to be small. This is because at the origin where $z = 0$ and $\rho = 0$, the effect of the in-plane field components add while that of the axial field components of the two counter-propagating beams largely cancel out. Hence the effect of the axial component which comes into play in the non-paraxial regime are negligible.

Any experimental work on this physical system will require looking into the effects of jitter and beam misalignment, among other detrimental factors. Jitter will no doubt pose an experimental challenge for the realization of sub-wavelength optical trapping potentials. Fortunately laser beam jitter has been and continues to be the subject of investigations which seek to find remedies by minimising or even eliminating laser beam jitter using adaptive optics [27, 28] In our particular physical set up the axial jitter is expected to mainly affect the focal planes shift parameter d. However, Fig. 4 (d) shows that the d-dependence of the axial force constant has a maximum magnitude in the trapping region near d $0.5w_0$. This suggests that in an experimental investigation the effect of axial jitter is minimized by choosing that d-value.

We note that the effective potential we are able to manipulate is located within a region of space of sub-wavelength dimensions which means that we are able to deal with a very localized potential that can be modified by changes of the parameters and this is done with or without the presence of other means of confinement.

Since our scheme involves counter propagating beams it can combine efficient cooling of the molasses type of an atomic cloud [1] along with its trapping. This is analogous to what happens in a magneto-optical trap (MOT) but without the use of a magnetic field. An order of magnitude analysis is as follows with reference to the results shown in Fig. 4 (c) and (d) where both the axial and radial force constants are negative. Assuming $d = w_0$ the force constant magnitudes are approximately -5.0×10^{-14} Nm^{-1} (axial) and -1.0×10^{-14} Nm^{-1} (radial). We also assume an intensity of 10.0 Wm^{-2} and take the detuning to be $-2\pi \times 10^7$ s^{-1} which ensures a low saturation parameter s=0.1 (a prerequisite condition for the realisation of optical molasses. These are four orders of magnitude larger than the force constant values in an MOT and our preliminary calculations with these parameters indicate a very stiff atom trapping.

ACKNOWLEDGEMENTS

KK is grateful to Tubitak as well as Bitlis Eren University, Turkey, for financial support during his sabbatical year which was hosted at the University of York, where this work was initiated.

DISCLOSURES

The authors declare no conflicts of interest.

REFERENCES

1. H. Metcalf and P. van der Straten, *Laser Cooling and Trapping*, Graduate Texts in Contemporary Physics (Springer New York, 2001).
2. C. Adams and E. Riis, "Laser cooling and trapping of neutral atoms," Prog. quantum electronics **21**, 1–79 (1997).
3. S. Chu, J. E. Bjorkholm, A. Ashkin, and A. Cable, "Experimental Observation of Optically Trapped Atoms," Phys. Rev. Lett. **57**, 314–317 (1986).
4. T. W. Hänsch and A. L. Schawlow, "Cooling of gases by laser radiation," Opt. Commun. **13**, 68–69 (1975).
5. D. E. Pritchard, E. L. Raab, V. Bagnato, C. E. Wieman, and R. N. Watts, "Light Traps Using Spontaneous Forces," Phys. Rev. Lett. **57**, 310–313 (1986).
6. A. Ashkin, "Trapping of Atoms by Resonance Radiation Pressure," Phys. Rev. Lett. **40**, 729–732 (1978).
7. V. G. Minogin, "Resonance-radiation pressure on atoms in symmetrical light fields," Opt. Lett. **10**, 179 (1985).
8. M. Babiker, D. L. Andrews, and V. E. Lembessis, "Atoms in complex twisted light," J. Opt. **21**, 013001 (2018).
9. T. Mashimo, M. Abe, and S. Tojo, "Effective trapping of cold atoms using dipole and radiative forces in an optical trap," Phys. Rev. A **100**, 063426 (2019).
10. A. Ashkin and J. P. Gordon, "Stability of radiation-pressure particle traps: an optical Earnshaw theorem," Opt. Lett. **8**, 511 (1983).
11. S. Earnshaw, "On the Nature of the Molecular Forces which Regulate the Constitution of the Luminiferous Ether," Trans. Camb. Phil. Soc. **7**, 97–114 (1842).
12. A. Ashkin, "Stable radiation-pressure particle traps using alternating light beams," Opt. Lett. **9**, 454 (1984).
13. S. Sukhov and A. Dogariu, "Non-conservative optical forces," Reports on Prog. Phys. **80**, 112001 (2017).
14. P. Woźniak, P. Banzer, F. Bouchard, E. Karimi, G. Leuchs, and R. W. Boyd, "Tighter spots of light with superposed orbital-angular-momentum beams," Phys. Rev. A **94**, 021803 (2016).

15. H. F. Schouten, T. D. Visser, and D. Lenstra, "Optical vortices near sub-wavelength structures," J. Opt. B: Quantum Semiclassical Opt. **6**, S404 (2004).
16. T. Bauer, P. Banzer, F. Bouchard, S. Orlov, L. Marrucci, E. Santamato, R. W. Boyd, E. Karimi, and G. Leuchs, "Multi-twist polarization ribbon topologies in highly-confined optical fields," New J. Phys. **21**, 053020 (2019).
17. R. Dorn, S. Quabis, and G. Leuchs, "Sharper focus for a radially polarized light beam," Phys. Rev. Lett. **91**, 1–4 (2003).
18. V. V. Kotlyar, S. S. Stafeev, and A. G. Nalimov, *Sharp Focusing of Laser Light* (CRC Press, 2019).
19. C. Cohen-Tannoudji and D. Guery-Odelin, *Advanced in atomic physics - an introduction* (World Scientific, New Jeresey, 2011).
20. R. J. Cook, "Atomic motion in resonant radiation: An application of Ehrenfest's theorem," Phys. Rev. A **20**, 224–228 (1979).
21. V. G. Minogin, "Theory of a radiative atomic trap," Sov. J. Quantum Electron. **12**, 299–303 (1982).
22. A. Ashkin, "Acceleration and Trapping of Particles by Radiation Pressure," Phys. Rev. Lett. **24**, 156–159 (1970).
23. K. Koksal, V. E. Lembessis, J. Yuan, and M. Babiker, "Interference of axially-shifted laguerre–gaussian beams and their interaction with atoms," J. Opt. **21**, 104002 (2019).
24. A. Ashkin, J. M. Dziedzic, J. E. Bjorkholm, and S. Chu, "Observation of a single-beam gradient force optical trap for dielectric particles," Opt. Lett. **11**, 288 (1986).
25. V. E. Lembessis and M. Babiker, "Mechanical effects on atoms interacting with highly twisted Laguerre-Gaussian light," Phys. Rev. A **94**, 043854 (2016).
26. M. Lax, W. H. Louisell, and W. B. McKnight, "From Maxwell to paraxial wave optics," Phys. Rev. A **11**, 1365–1370 (1975).
27. H. Yoon, B. Bateman, and B. Agrawal, "Laser beam jitter control using recursive-least-squares adaptive filters," J. Dyn. Syst. Meas. Control. **133**, 041001 (2011).
28. J. Baker, F. Barone, E. Calloni, R. De Rosa, L. Fiore, A. Eleuteri, L. Milano, S. Restaino, and K. Quipiani, "An adaptive optics approach to the reduction of misalignments and beam jitters in gravitational wave interferometers," Class. Quantum Gravity - CLASS QUANTUM GRAVITY **19**, 1813–1818 (2002).